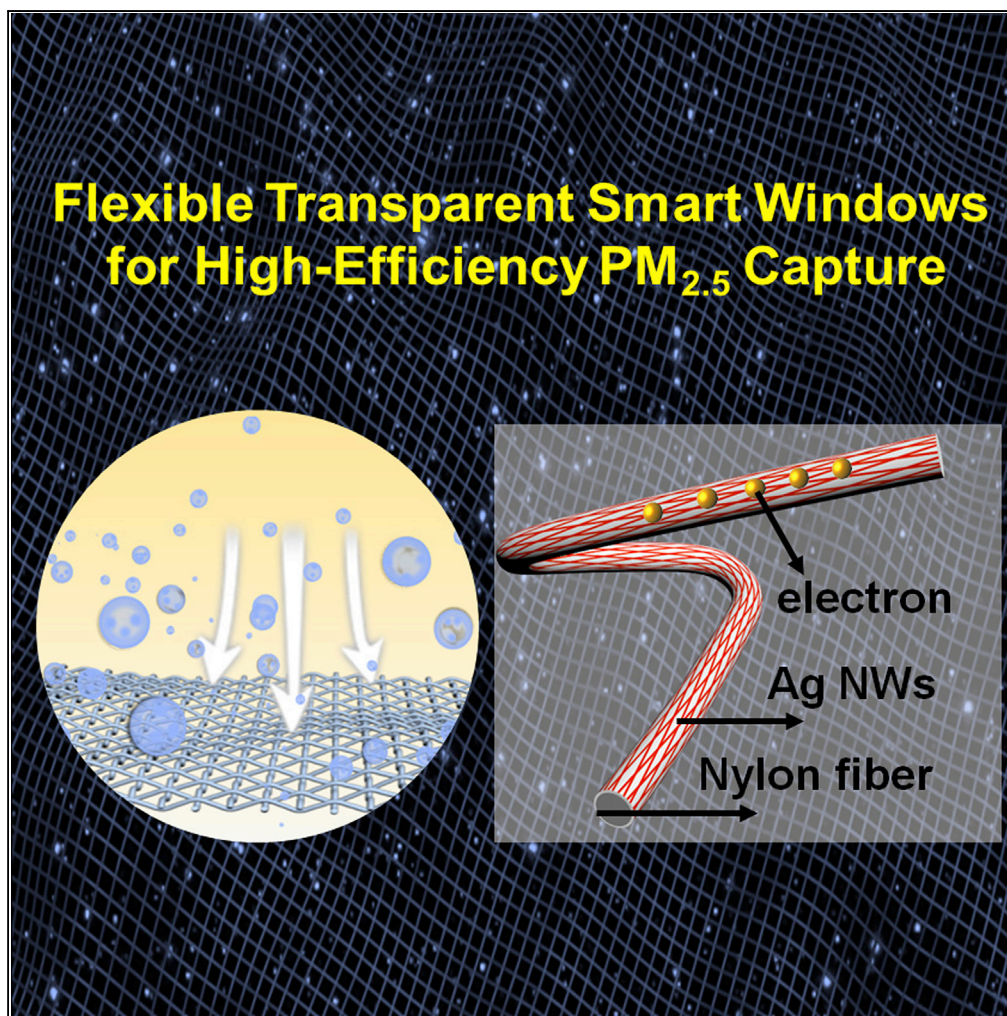


Article

Mass Production of Nanowire-Nylon Flexible Transparent Smart Windows for PM_{2.5} Capture

Wei-Ran Huang,
Zhen He, Jin-Long
Wang, Jian-Wei
Liu, Shu-Hong Yu

jwliu13@ustc.edu.cn (J.-W.L.)
shyu@ustc.edu.cn (S.-H.Y.)

HIGHLIGHTS

A large-area flexible transparent window with low resistance and high transmittance

The window can turn the indoor light intensity and capture fine particulate matter (PM_{2.5})

As a PM filter, the removal efficiency is high and the processing speed is fast

Huang et al., iScience 12, 333–341
February 22, 2019 © 2019 The Authors.
<https://doi.org/10.1016/j.isci.2019.01.014>

Article

Mass Production of Nanowire-Nylon Flexible Transparent Smart Windows for PM_{2.5} Capture

Wei-Ran Huang,¹ Zhen He,¹ Jin-Long Wang,¹ Jian-Wei Liu,^{1,*} and Shu-Hong Yu^{1,2,*}

SUMMARY

Designing large-area flexible transparent smart windows for high-efficiency indoor fine particulate matter (PM_{2.5}) capture is important to guarantee safe indoor environments. In this article, we demonstrate that large-area fabrication of flexible transparent Ag-nylon mesh can be performed not only to turn the indoor light illumination intensity as thermochromic smart windows after uniformly coating with thermochromic dye but also to purify indoor air as high-efficiency PM_{2.5} filter. It takes only about \$15.03 and 20 min to fabricate 7.5-m² Ag-nylon flexible transparent windows without any modification with a sheet resistance of as low as 8.87 Ω sq⁻¹ and optical transmittance of 86.05%. As an excellent PM filter (can be recycled after PM filtration), the removal efficiency is as high as 99.65% and the processing speed is high, which can reduce the PM_{2.5} density from heavily polluted (248 μg · m⁻³, purple alert) to good (32.9 μg · m⁻³, green statement) in 50 s.

INTRODUCTION

Flexible transparent electronics have drawn great attention because of their excellent performance both in mechanical flexibility and optical transmittance, which were widely used in screen display (Bae et al., 2010; Han et al., 2014; Bari et al., 2016), organic light-emitting diodes (Zhang et al., 2006; Wu et al., 2010; Lee et al., 2017), transparent supercapacitors (Moon et al., 2017; Lee et al., 2016), flexible transparent heaters (Hong et al., 2015; Ji et al., 2014), and solar cells (Wang et al., 2008; Lee et al., 2012). In recent years, a wide scope of strategies are available to construct flexible transparent electrodes for advanced electronics, such as the bubble template (Tokuno et al., 2012), the coffee ring effect template (Layani et al., 2009), polymer nanofiber template (Wu et al., 2013), nanowire (NW) assembly (Liu et al., 2013, 2014), roll-to-roll techniques (Bae et al., 2010), inkjet printing method (Jiang et al., 2016), and Mayer rod coating (Hu et al., 2010). However, these strategies can hardly meet the requirements of the many modern optoelectronic devices, because their fabrication processes highly rely on expensive scientific equipment or sophisticated material processing steps. In addition, these processes are complex with high cost and small area limitation, which greatly limit their wide applications. For example, de With et al. reported a solution-processed method to prepare large-area graphene film with an area of 50 cm² for conductive, flexible, and transparent electrodes, which showed conductivity of 800 Ω sq⁻¹ and transmittance of 45% at 500 nm wavelength (Arapov et al., 2015). Liu et al. reported a hexane-air-interface-induced assembly method to construct graphene oxide films for flexible and transparent electrodes with conductivity of 476 Ω sq⁻¹ and transmittance of 76% at 550 nm (50 cm²) (Fan et al., 2015).

Meanwhile, nearly all flexible transparent electrodes are constructed by coating conductive nano-building blocks (noble NWs, carbon nanotube, or graphene) on flexible substrates, which are windtight. Combining functional nanoscale building blocks with commercial skeleton not only lowers the cost of application but also does it in a way that manages to solve the major issues in the field of nanoscience and nanotechnology and accelerates the pace of practicability in reality. For example, commercial sponge was selected to combine with nanomaterials for oil spill remediation (Ge et al., 2014). In addition, carbon cloth (Liu et al., 2012) and graphene-based fibers (Zhou et al., 2018) were always used as electrodes for batteries and supercapacitors. That is, NW-nylon meshes are transparent, flexible, and porous; have strong affinity to air pollutants; and therefore show high removal efficiency at low pressure drop (Jeong et al., 2017).

Herein, we develop a simple strategy for the fabrication of large-area flexible transparent thermochromic smart windows for high-efficiency fine particulate matter (PM_{2.5}) capture (Lin et al., 2018; Liu et al., 2015). It takes only about \$15.03 and 20 min to fabricate 7.5-m² Ag-nylon electrodes in air without any modification

¹Division of Nanomaterials & Chemistry, Hefei National Laboratory for Physical Sciences at the Microscale, CAS Center for Excellence in Nanoscience, Collaborative Innovation Center of Suzhou Nano Science and Technology, Department of Chemistry, Hefei Science Center of CAS, University of Science and Technology of China, Hefei 230026, China

²Lead Contact

*Correspondence: jwliu13@ustc.edu.cn (J.-W.L.), shyu@ustc.edu.cn (S.-H.Y.)
<https://doi.org/10.1016/j.isci.2019.01.014>



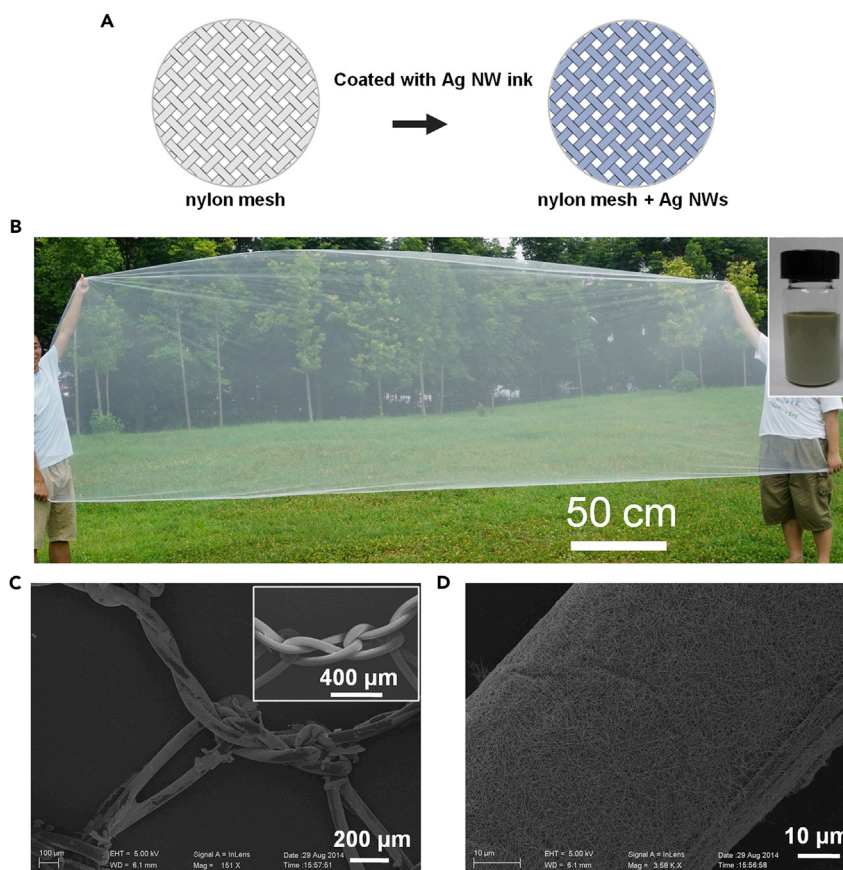


Figure 1. Flexible Transparent Conductive Ag-Nylon Electrodes

(A) Schematic illustration of the fabrication of conductive Ag-nylon electrodes.

(B) Photograph of a large-scale conductive nylon mesh. Inset: photograph of AgNW ink using ethanol as a solvent with a concentration of 3.92 mg mL^{-1} .

(C and D) SEM images of Ag-nylon meshes with different magnifications. Inset: SEM image of initial nylon meshes without any AgNWs.

having a sheet resistance of as low as $8.87 \Omega \text{ sq}^{-1}$ with 86.05% optical transmittance, and it is easy for us to further expand production (Table S1 in Supplemental Information). The time-dependent temperature profiles and uniform heat distribution show that the obtained Ag-nylon electrodes can be used as an ideal intelligent thermochromic smart window with excellent mechanical stability whose performance remains stable even after 10,000 bending cycles of bending test with a minimum bending radius of 2.0 mm and 1,000 cycles of stretching deformation with mechanical strain as high as 10%. In addition, the Ag-nylon electrodes can be constructed for PM filter showing a removal efficiency of 99.65% and maintaining stable even after 100 cycles of PM filtration and cleaning process.

RESULTS

Fabrication of Ag-Nylon Electrodes

Our approach for producing large-area Ag-nylon NW electrodes is through a one-step coating process using commercially available nylon cloth as substrate and Ag NW ethanol solution as ink, which is illustrated in Figure 1A (Video S1 in Supplemental Information). First, high-quality Ag NWs with diameter 60–80 nm and length 20 μm (Figure S1) were synthesized using the polyol growth process reported previously by Yang et al. with some modifications (Yang et al., 2011). Before the fabrication procedure, commercial nylon was cleaned with alcohol and then acetone, then subjected to ultrasonic treatment for 30 min, and dried at 60°C . Subsequently, Ag NW ethanol solution with a concentration of 3.92 mg mL^{-1} (inset of Figure 1B) was used as a conductive ink to dye the nylon mesh to construct large-area (7.5 m^2) conductive and transparent electrodes (Figure 1B). After full infiltration in the Ag NW ethanol solution, the bare nylon mesh was

gradually coated with a film of Ag NWs with increasing dipping cycles, owing to the hydrophilic surface of both the nylon fiber and Ag NWs. From scanning electron microscopic (SEM) images in Figures 1C and 1D, it is found that the distribution of Ag NWs on the fiber is very uniform. The whole preparation process is simple and is feasible to operate in air at room temperature. In addition, it does not need special apparatus and is suitable for mass production and promotion with low cost (see Cost accounting of Ag-nylon electrodes in Supplemental Information).

Optical Transmittance and Electrical Conductivity of Ag-Nylon Electrodes

The optical transmittance and electrical conductivity of the obtained Ag-nylon electrodes can be optimized by controlling the density of the Ag NW coating on the surface of the nylon skeleton by tuning the number of dip-coating cycles or the concentration of the AgNW solution. After annealing at 140°C for 15 min (Figures S2 and S3), the transmittance and sheet resistance were recorded by UV-2501PC/2550 (Shimadzu Corporation, Japan) and PM5 Analytical Probe System (Cascade Microtech, Inc.) coupled with a Keithley 4200 SCS in a metal-shielded box with four-point probes in which the sheet resistance values were the average of 10 measurements on the same sample. Figure 2A shows the optical transmittance of the Ag-nylon networks with the Ag NW ink concentration of 3.92 mg mL⁻¹ for different dipping cycles. It is well known that 550 nm is the mean wavelength of visible light and is the most sensitive wavelength region for human beings. The optical transmittance of bare nylon mesh without any Ag NW coating is about 98.8% at 550 nm. During the first 10 dipping cycles (cycles 1, 2, 3, 4, 6, 8, and 10), the transmittance changed from 95.02% to 92.79%, 91.35%, 88.20%, 86.05%, 83.54%, and 81.40%, respectively. The corresponding electrical conductivities of the Ag-nylon electrodes during the dipping process are shown in the inset of Figures 2A and 2B. With an increase in dipping cycles and keeping the concentration of Ag NW ink constant, the conductivities of the Ag-nylon electrodes become higher, showing a gradual drop in the transmittance during the first 10 cycles. For the sixth dip-coating cycle of Ag-nylon mesh, the transmittance was 86.05% while the sheet resistance was 8.87 Ω sq⁻¹, indicating that the conductive Ag-nylon electrodes can combine excellent transmittance with low sheet resistance, which are much better than those of 80-nm indium tin oxides (ITO, 85%, 62 Ω sq⁻¹) (Kim et al., 1999). The electrical conductivity of the Ag-nylon network can be also tuned by changing the concentration of the Ag NW solution (Figure 2B). When the concentration of the Ag NW solution changes from 3.92 mg mL⁻¹ to 12.08 mg mL⁻¹, the sheet resistance of mesh can achieve 341.25 Ω sq⁻¹ after two dip-coating processes and decreases to 1.40 Ω sq⁻¹ quickly in 10 dip-coating cycles. Figure 2C illustrates the change in transmittance and conductivity of Ag-nylon electrodes as a function of the mass content. It is found that the transmittance and sheet resistance decrease almost linearly with the increase of the mass content of Ag NWs. Figure 2D depicts the sheet resistance versus optical transmittance (at 550 nm) of the Ag-nylon transparent conductive electrodes reported here and Ag networks prepared by other different methods (Bae et al., 2010; Han et al., 2014; Hu et al., 2010; Guo et al., 2013). It is indicated that the obtained conductive Ag-nylon electrodes achieve better transmittance and conductivity than many other materials, such as Ag NW electrode (81.7%, 38 Ω sq⁻¹) (Hu et al., 2010), Cu NW electrode (78.1%, 23.3 Ω sq⁻¹) (Guo et al., 2013), and Au nanomesh (82.5%, 20 Ω sq⁻¹) (Guo et al., 2014).

Mechanistic Investigation of Ag-Nylon Electrodes

It is well known that mechanical flexibility and stability are two important factors for the long life of flexible transparent electronics. The obtained Ag-nylon transparent electrodes exhibit a constant resistance, which shows almost no degradation even after 10,000 cycles of fatigue test with a minimum bending radius of 2.0 mm, indicating their excellent mechanical flexibility and stability. Figure 2E shows that the resistance value was constant during the cyclic bending test, which was carried out with a high-precision mechanical system (Instron 5565A) and a Keithley 4200 SCS in a clean, metal-shielded box. To test the stability of the Ag-nylon flexible transparent electrodes, fatigue test was carried out in Figure 2F, which shows good conductivity with electrical resistance only changing from 15.2 to 19.3 Ω after more than 10,000 bending cycles indicating its excellent stability and reversibility. Moreover, the Ag-nylon transparent electrodes depict outstanding stretchable properties. It was found that the structure and resistance of the Ag-nylon transparent electrodes show no degradation during the 10% tension deformation even after 1,000 stretching cycles (Figure S4), which is better than those of traditional ITO heater and graphene-based heaters, which can only endure 1.10% and 4.0% tensile strain, respectively (Kang et al., 2011).

Intelligent Thermo-chromic Window

The intelligent thermo-chromic window can change its color or transmittance in response to thermal stimulus (Parkin and Manning, 2006; Seeboth et al., 2014). Ko et al. even combined the thermo-chromic dye with

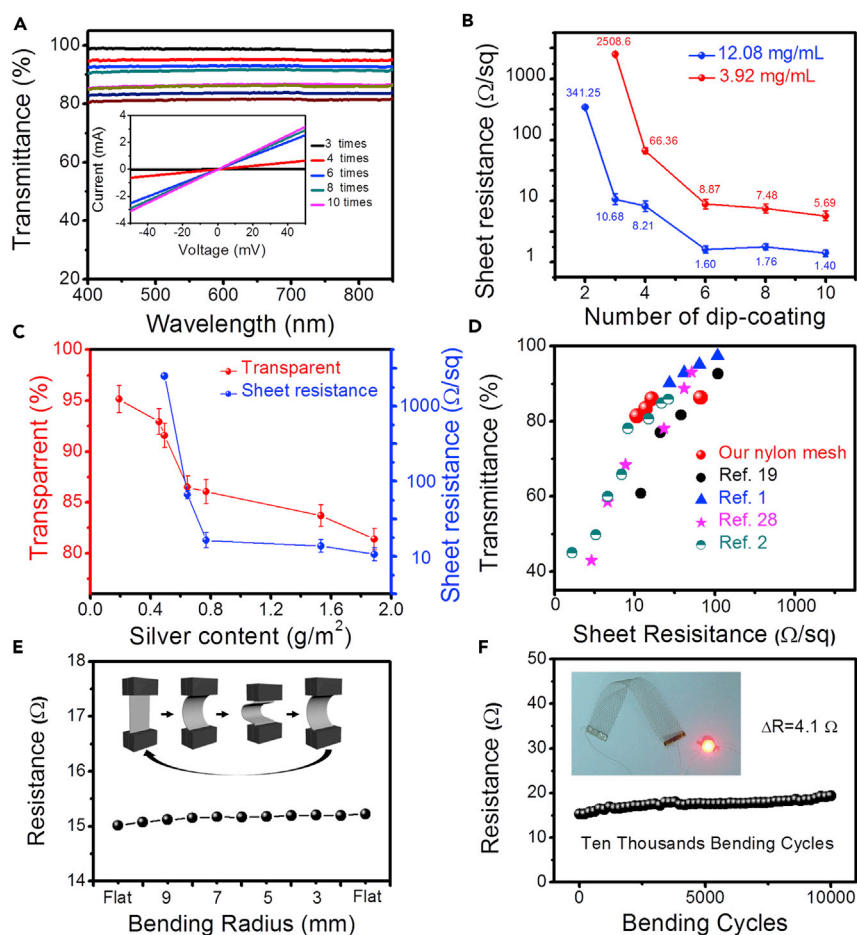


Figure 2. Optical Transmittance, Electrical Conductivity, and Mechanical Performance of Ag-Nylon Electrodes
 (A) Optical transmittance of the Ag-nylon electrodes with different dipping cycles with AgNW solution concentration of 3.92 mg mL^{-1} . From top to bottom, the numbers of dipping cycles are 0, 1, 2, 3, 4, 6, 8, and 10. Inset: current-voltage characteristic of conductive Ag-nylon electrodes with different dipping cycles.
 (B) Sheet resistance of conductive Ag-nylon electrodes as a function of different dip-coating cycles when the concentration is 3.92 mg mL^{-1} and 12.08 mg mL^{-1} .
 (C) Silver content as a function of sheet resistance and optical transmittance of Ag-nylon electrodes.
 (D) Comparison of sheet resistance and transmittance taken from our work and other reported references.
 (E) Electrical resistance change as a function of the different degrees of bending in the first bending cycle at a bending radius of up to 2.0 mm. Inset: schematic illustration of the cyclic bending test under mechanical deformation.
 (F) Ag-nylon electrodes keep stable during 10,000 bending cycles. Inset: photograph of flexible conductive nylon meshes completing an electrical circuit with a power source and a red light-emitting diode. Error bars correspond to the average taken over at least 30 measurements.

biomimetic color-changing and soft robotics (Kim et al., 2018). Ag-nylon electrodes with high heating efficiency when applying a direct voltage were selected as the skeleton to fabricate reversibly flexible thermochromic smart windows by spraying thermochromic dye dispersed in acetone at 60°C , as demonstrated in Figure 3. After direct voltage is applied to the Ag-nylon electrodes ($R_s = 4.2 \Omega \text{ sq}^{-1}$, valid heating area: $50 \text{ mm} \times 50 \text{ mm}$), the surface temperature increases over time until reaching a steady-state temperature is reached, as shown in Figure 3A. It is found that higher applied voltages result in faster heating rate, and the steady-state temperature of the Ag-nylon conductive mesh increases obviously with a slight increase of the applied voltage from the time-dependent temperature profiles. In detail, the steady-state temperature rises from 33.3°C , 42.6°C , 54.4°C , 71.0°C , 82.5°C to 105.1°C , when the corresponding applied voltages are 1.0 V, 1.5 V, 2.0 V, 2.5 V, 3.0 V, and 3.5 V, which is much smaller than those of most traditional nanostructured heaters, such as graphene film (60 V) (Sui et al., 2011), trilayer graphene film (30 V) (Bae et al., 2012), single-walled carbon nanotube film (12 V) (Yoon et al., 2007), Ag NW film (7 V) (Kim et al., 2013), and Ag

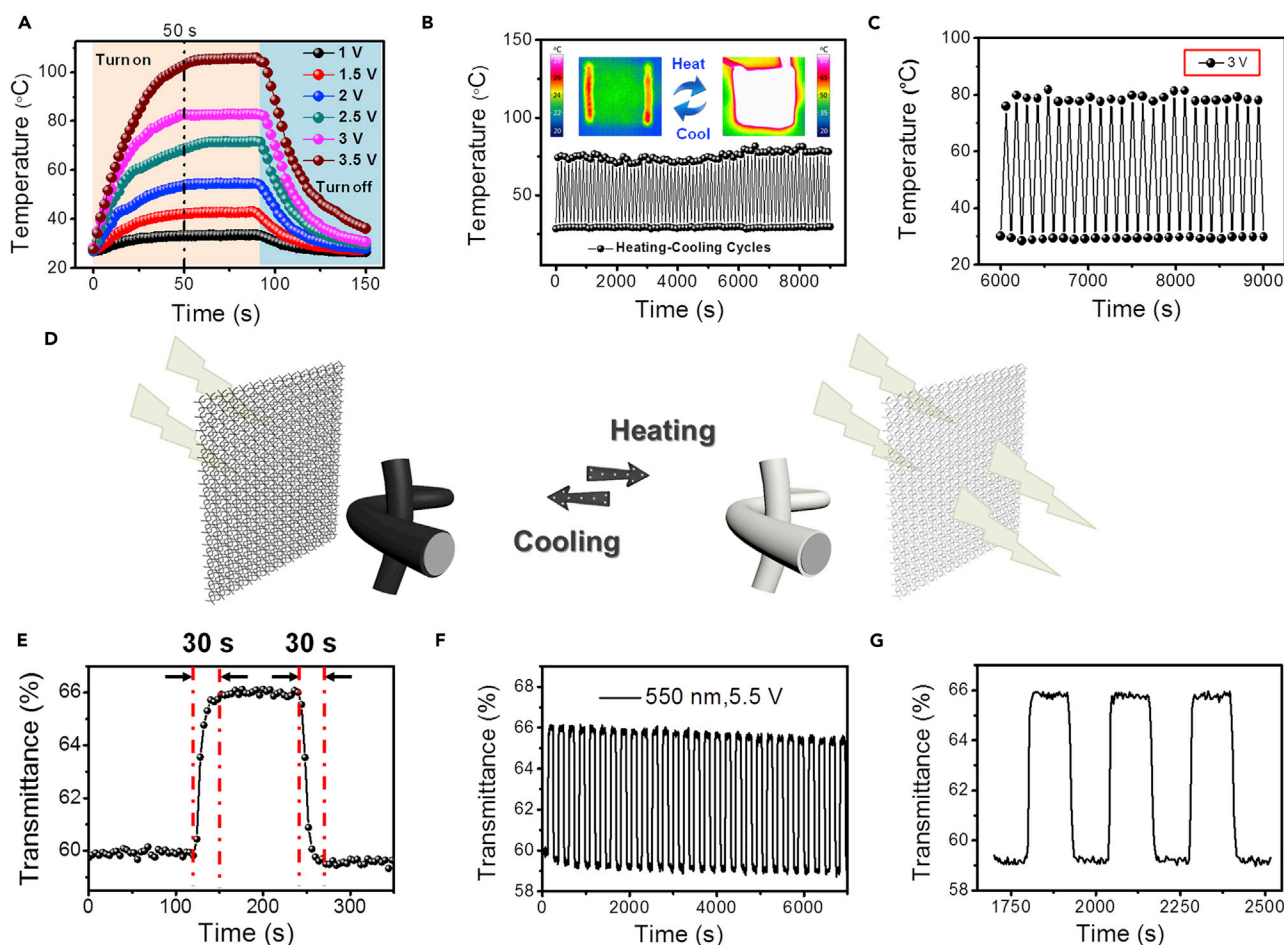


Figure 3. Ag-Nylon Flexible Transparent Thermochromic Windows

(A) Time-dependent temperature profiles of flexible transparent Ag-nylon films with different applied voltage.

(B) Reversible temperature switching of the Ag-nylon films. Inset: infrared pictures between heating and cooling states.

(C) Enlarged plots from 6,000 to 9,000 s.

(D) Illustration of the thermochromic process.

(E–G) Thermochromic switching performance of Ag-nylon windows. (E) Response time of a single thermochromic test. (F) Thermochromic switching test for 7,000 s. (G) Enlarged plots from 1,700 to 2,500 s.

NWs/PEDOT:PSS film (6 V) (Ji et al., 2014). Most importantly, the response time from room temperature to the steady-state temperature of Ag-nylon electrodes (50 s) is shorter by 83.33% than that of graphene (300 s) (Bae et al., 2012), by 16.67% than that of the Ag NWs (60 s) (Kim et al., 2013), and by 50% than that of the Ag NWs/poly(3,4-ethylenedioxythiophene):poly(styrenesulfonate) (PEDOT:PSS) film (100 s) (Ji et al., 2014). To further control the heating property of the Ag-nylon substrate, continuous square-wave voltages are applied, from 1.0 V, 1.5 V, 2.0 V, 2.5 V, 3.0 V, 3.5 V to 4.0 V. As expected, the temperature experiences an orbit of regular echelon rising as shown in Figure S5. Electric pulses (pulse width = 60 s, +3 V) were applied, and Figures 3B and 3C show that the devices give fairly reproducible results for the high- and low-temperature switching phenomena. After long-time switching cycles, the temperature of the electrode remains uniform in the whole area (inset of Figure 3B) and is very sensitive to the input voltage (dynamic response to temperature), showing no degradation. In addition, as a versatile strategy, various Ag-nylon electrode patterns, such as a circle, square ring, triangular ring, and rectangular ring, were designed showing a uniform heating performance and flexible way to manipulate the heating area (Figure S6). After uniformly coating with thermochromic dye (Figure S7), the flexible Ag-nylon thermochromic film shows reversible transmittance switching when the input voltage is on and off (Figure 3D). When a direct voltage of 5.5 V is applied, it takes 30 s to change its color from black to white (or change black to white) (Figure 4E, Video S2 in Supplemental Information), which is much faster than the previous reports, such as

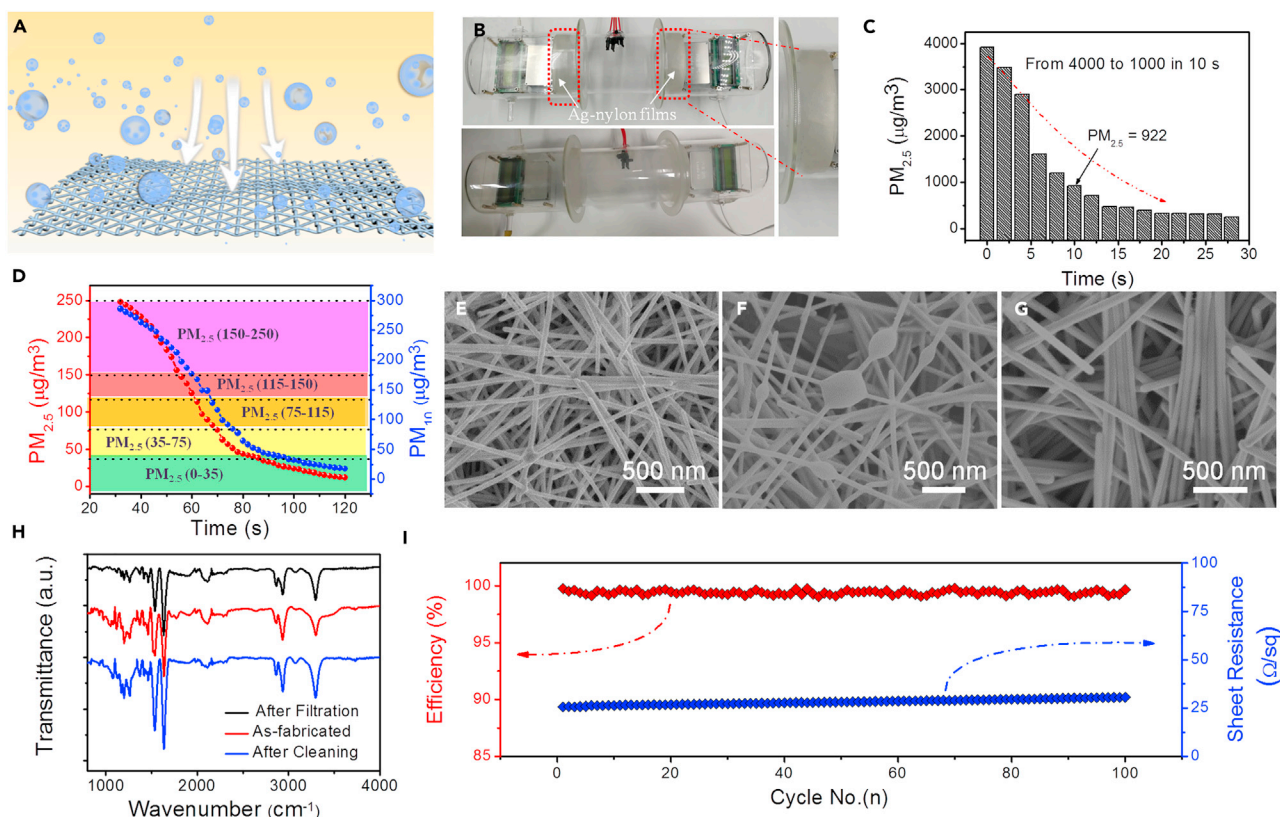


Figure 4. PM Filtration of Flexible Transparent Ag-nylon Windows

- (A) Schematic diagram illustrating the PM filtration process.
- (B) Optical photograph of the experimental setup for PM capture.
- (C) Evolution of $PM_{2.5}$ densities in real time from 0 to 30 s under an applied voltage of 10 V.
- (D) Evolution of $PM_{2.5}$ and PM_{10} densities from 30 to 120 s under the same voltage.
- (E–G) SEM images of Ag-nylon film as PM filter for (E) as-fabricated, (F) after PM filtration, and (G) after cleaning process, respectively.
- (H) Corresponding FTIR spectra of as-fabricated PM filter, PM filter after filtration, and recycled PM filter.
- (I) Recycled PM filter for 100 cycles.

$TiO_2(R)/VO_2(M)/TiO_2(A)$ multilayer film (180 s) (Zheng et al., 2015), VO_2/TiN smart coatings (150 s) (Hao et al., 2018), and single-walled nanotube/ VO_2 /mica hierarchical films (50 s) (Chen et al., 2017a). More importantly, from the first cycle to long-time cycles (Figures 3F and 3G), on-off ratio remains almost consistent (100%) with no degradation, suggesting a stable reversible thermochromic smart window.

High-Efficiency $PM_{2.5}$ Capture

The obtained large-area Ag-nylon thermochromic smart windows also show potentials for high-efficiency $PM_{2.5}$ capture. As we know, particle pollution in air is one of the most serious issues that may cause diseases, allergies, and also death of humans or other living organisms such as animals and food crops. Many novel methods have been reported to reduce the density of PM in air, such as static electricity adsorption (Jeong et al., 2017; Gu et al., 2017; Han et al., 2015), polymer fiber filtration (Liu et al., 2015; Khalid et al., 2017; Xu et al., 2016; Zhang et al., 2016), and metal-organic framework materials (Chen et al., 2017b). Seung's group reported a work in the field of $PM_{2.5}$ filtration by employing the negative ionizer to reduce the applied voltage (Jeong et al., 2017). Figures 4A and 4B show the PM filtration process and experimental setup, while the close-up view on the lower right in Figure 4B shows the transparent Ag-nylon windows. The PM counter sensors placed at the left and right sides of the chamber record the PM density at the inlet and outlet, respectively. In the center of the chamber, a negative ionizer was placed to charge the PM. The flexible transparent Ag-nylon windows as PM filters were inserted at both ends of the chamber to collect and remove PM in the air. Before starting the experiment, PM filled the left side of the chamber by burning sandalwood. Then, sanders continuously

produced PM particles to the left side of the chamber near the negative ionizer. After ionization by the negative ionizer, a stable voltage of 10 V was applied to the Ag-nylon films. Figures 4C and 4D show the evolution of PM densities in real time under the applied voltage of 10 V. Using our Ag-nylon windows, it takes only 10 s to reduce the density of the PM_{2.5} from 3,922 $\mu\text{g}\cdot\text{m}^{-3}$ to 922 $\mu\text{g}\cdot\text{m}^{-3}$. More importantly, the PM_{2.5} density was reduced from heavily polluted (248 $\mu\text{g}\cdot\text{m}^{-3}$, purple alert) to good (32.9 $\mu\text{g}\cdot\text{m}^{-3}$, green statement) after only 50 s (less than 1 min) while the PM₁₀ density change followed the similar trends as shown in Figure 4D. As a result, the efficiency of Ag-nylon windows for PM capture was more than 99.65%, which is better than those of numerous reported ones, such as polymer nanofiber filter (98.69%) (Liu et al., 2015), ZIF-8@glass cloth (96.8%) (Chen et al., 2017b), blow-spinning of nanofibers (99%) (Khalid et al., 2017), and triboelectric nanogenerator enhanced nanofiber air filters (90.6%) (Gu et al., 2017). On the other hand, the Ag-nylon windows can be recycled after PM filtration just by cleaning in the ethanol for 20 min as shown in Figures 4E–4G, S8, and S9. An obvious yellowish-brown area appeared at the center of Ag-nylon electrode after PM filtration and disappeared after the cleaning process (Figure S10). The collected particles were completely removed by the simple washing process, which was further confirmed by the corresponding Fourier transform infrared (FTIR) spectra (Figure 4H) and X-ray photoelectron spectroscopic (XPS) analysis (Figure S11). It was found that the obviously weakened signals from 1,000 cm^{-1} to 1,200 cm^{-1} in FTIR spectra and obviously weakened C=O bond at 287.7 eV and N-C bond at 399.5 eV in XPS patterns were reinforced again after the washing process. The excellent PM capture performance and reusability of the Ag-nylon windows were further demonstrated by the long-time recycling (Figure 4I). After 100 cycles of PM_{2.5} capture, the removing efficiency (99.65%) and the sheet resistance of the Ag-nylon windows remained stable without obvious property degradation. Last but not least, thanks to the mass production ability of the Ag-nylon electrodes, we can easily expand the space for PM_{2.5} removal. For example, a 0.5 × 0.5-m² Ag-nylon window was selected to treat air pollution in a large cube with side length of 0.5 m (Figure S12) and the efficiency was still as high as 99.48%, indicating that the smart windows show real potential for indoor PM_{2.5} capture. As shown in Figure S13, flexible transparent Ag-nylon windows also have a very low pressure drop of 14.43 Pa at gas velocity of 0.2 m/s. It ensures the excellent ventilation of PM_{2.5} capture in daily life.

DISCUSSION

In conclusion, we demonstrate a versatile strategy for large-area fabrication of Ag-nylon electrode (7.5 m²) in 20 min with an optical transmittance of 86.05% and conductivity of 8.87 Ωsq^{-1} for high-performance thermochromic smart windows and PM_{2.5} capture. The flexible transparent and stretchable intelligent thermochromic smart window with uniform NW coating enables reversible color change with fast response time under low direct voltage stimulus. More importantly, the large-area Ag-nylon smart window exhibits excellent PM_{2.5} removal performance that mainly comes from four features. First, it has a high removal efficiency of 99.65%. It takes only 50 s to reduce the PM_{2.5} density from heavily polluted (248 $\mu\text{g}\cdot\text{m}^{-3}$, purple alert) to good (32.9 $\mu\text{g}\cdot\text{m}^{-3}$, green statement). Second, the Ag-nylon windows can be recycled after PM filtration just by dipping in ethanol for 20 min. There is no removal efficiency degradation after 100 cycles of reuse. Third, it is easy to expand the space for PM_{2.5} capture; for example, the removal efficiency remains up to 99.48% when the volume increases to 0.5 m × 0.5 m × 0.5 m. Finally, such a material shows excellent mechanical stability. The structure and performance remain stable even after 10,000 bending cycles of bending test with a minimum bending radius of 2.0 mm and 1,000 cycles of stretching deformation with mechanical strain as high as 10%. The success of the present design strategy provides more choices in developing next-generation flexible transparent smart windows and air pollution filters.

Limitations of Study

We have designed and fabricated Ag-nylon meshes as flexible transparent smart windows for PM_{2.5} capture. Ag NWs are not very stable in air due to the reaction with S element in the atmosphere. The electrodes would become a little pale yellow after 1 year of exposure to air.

METHODS

All methods can be found in the accompanying [Transparent Methods supplemental file](#).

SUPPLEMENTAL INFORMATION

Supplemental Information includes Transparent Methods, 13 figures, 1 table, and 2 videos and can be found with this article online at <https://doi.org/10.1016/j.isci.2019.01.014>.

ACKNOWLEDGMENTS

We acknowledge the funding support from the National Natural Science Foundation of China (grants 21761132008, 21771168, 21431006, 51471157, and 21403204), the Foundation for Innovative Research Groups of the National Natural Science Foundation of China (grant 21521001), Key Research Program of Frontier Sciences, CAS (grant QYZDJ-SSW-SLH036), the National Basic Research Program of China (grant 2014CB931800, 2013CB931800), and the Users with Excellence and Scientific Research Grant of Hefei Science Center of CAS (2015HSC-UE007) and the Fundamental Research Funds for the Central Universities (WK2100000005). This work was partially carried out at the USTC Center for Micro and Nanoscale Research and Fabrication.

AUTHOR CONTRIBUTIONS

S.-H.Y. conceived and designed the experiments. S.-H.Y. and J.-W.L supervised the research. W.-R.H., Z.H., and J.-L.W. carried out the experiments and characterizations. W.-R.H., Z.H., J.-L.W., J.-W.L., and S.-H.Y. analyzed the data and co-wrote the manuscript.

DECLARATION OF INTERESTS

The authors declare that they have no conflicts of interest with the contents of this article.

Received: October 26, 2018

Revised: December 23, 2018

Accepted: January 8, 2019

Published: February 22, 2019

REFERENCES

- Arapov, K., Goryachev, A., de With, G., and Friedrich, H. (2015). A simple and flexible route to large-area conductive transparent graphene thin-films. *Synth. Met.* *201*, 67–75.
- Bae, S., Kim, H., Lee, Y., Xu, X.F., Park, J.S., Zheng, Y., Balakrishnan, J., Lei, T., Kim, H.R., Song, Y.J., et al. (2010). Roll-to-roll production of 30-inch graphene films for transparent electrodes. *Nat. Nanotechnol.* *5*, 574–578.
- Bae, J.J., Lim, S.C., Han, G.H., Jo, Y.W., Doung, D.L., Kim, E.S., Chae, S.J., Ta Quang, H., Nguyen Van, L., and Lee, Y.H. (2012). Heat dissipation of transparent graphene defoggers. *Adv. Funct. Mater.* *22*, 4819–4826.
- Bari, B., Lee, J., Jang, T., Won, P., Ko, S.H., Alamgir, K., Arshad, M., and Guo, L.J. (2016). Simple hydrothermal synthesis of very-long and thin silver nanowires and their application in high quality transparent electrodes. *J. Mater. Chem. A* *4*, 11365–11371.
- Chen, Y.L., Fan, L.L., Fang, Q., Xu, W.Y., Chen, S., Zan, G.B., Ren, H., Song, L., and Zou, C.W. (2017a). Free-standing SWNTs/VO₂/Mica hierarchical films for high-performance thermochromic devices. *Nano Energy* *31*, 144–151.
- Chen, Y., Zhang, S., Cao, S., Li, S., Chen, F., Yuan, S., Xu, C., Zhou, J., Feng, X., Ma, X., et al. (2017b). Roll-to-roll production of metal-organic framework coatings for particulate matter removal. *Adv. Mater.* *29*, 1606221.
- Fan, T.J., Yuan, C.Q., Tang, W., Tong, S.Z., Liu, Y.D., Huang, W., Min, Y.G., and Epstein, A.J. (2015). A novel method of fabricating flexible transparent conductive large area graphene film. *Chin. Phys. Lett.* *32*, 076802.
- Ge, J., Ye, Y.D., Yao, H.B., Zhu, X., Wang, X., Wu, L., Wang, J.L., Ding, H., Yong, N., and He, L.H. (2014). Pumping through porous hydrophobic/oleophilic materials: an alternative technology for oil spill remediation. *Angew. Chem. Int. Ed.* *53*, 3612–3616.
- Gu, G.Q., Han, C.B., Lu, C.X., He, C., Jiang, T., Gao, Z.L., Li, C.J., and Wang, Z.L. (2017). Triboelectric nanogenerator enhanced nanofiber air filters for efficient particulate matter removal. *ACS Nano* *11*, 6211–6217.
- Guo, H.Z., Lin, N., Chen, Y.Z., Wang, Z.W., Xie, Q.S., Zheng, T.C., Gao, N., Li, S.P., Kang, J.Y., Cai, D.J., et al. (2013). Copper nanowires as fully transparent conductive electrodes. *Sci. Rep.* *3*, 2323.
- Guo, C.F., Sun, T.Y., Liu, Q.H., Suo, Z.G., and Ren, Z.F. (2014). Highly stretchable and transparent nanomesh electrodes made by grain boundary lithography. *Nat. Commun.* *5*, 3121.
- Han, B., Pei, K., Huang, Y.L., Zhang, X.J., Rong, Q.K., Lin, Q.G., Guo, Y.F., Sun, T.Y., Guo, C.F., Carnahan, D., et al. (2014). Uniform self-forming metallic network as a high-performance transparent conductive electrode. *Adv. Mater.* *26*, 873–877.
- Han, C.B., Jiang, T., Zhang, C., Li, X., Zhang, C., Cao, X., and Wang, Z.L. (2015). Removal of particulate matter emissions from a vehicle using a self-powered triboelectric filter. *ACS Nano* *9*, 12552–12561.
- Hao, Q., Li, W., Xu, H.Y., Wang, J.W., Yin, Y., Wang, H.Y., Ma, L.B., Ma, F., Jiang, X.C., Schmidt, O.G., et al. (2018). VO₂/TiN plasmonic thermochromic smart coatings for room-temperature applications. *Adv. Mater.* *30*, 1705421.
- Hong, S., Lee, H., Lee, J., Kwon, J., Han, S., Suh, Y.D., Cho, H., Shin, J., Yeo, J., and Ko, S.H. (2015). Highly stretchable and transparent metal nanowire heater for wearable electronics applications. *Adv. Mater.* *27*, 4744–4751.
- Hu, L., Kim, H.S., Lee, J.-Y., Peumans, P., and Cui, Y. (2010). Scalable coating and properties of transparent, flexible, silver nanowire electrodes. *ACS Nano* *4*, 2955–2963.
- Jeong, S., Cho, H., Han, S., Won, P., Lee, H., Hong, S., Yeo, J., Kwon, J., and Ko, S.H. (2017). High efficiency, transparent, reusable, and active PM_{2.5} filters by hierarchical Ag nanowire percolation network. *Nano Lett.* *17*, 4339–4346.
- Ji, S., He, W., Wang, K., Ran, Y., and Ye, C. (2014). Thermal response of transparent silver nanowire/PEDOT: PSS film heaters. *Small* *10*, 4951–4960.
- Jiang, J.K., Bao, B., Li, M.Z., Sun, J.Z., Zhang, C., Li, Y., Li, F.Y., Yao, X., and Song, Y.L. (2016). Fabrication of transparent multilayer circuits by inkjet printing. *Adv. Mater.* *28*, 1420–1426.
- Kang, J., Kim, H., Kim, K.S., Lee, S.K., Bae, S., Ahn, J.H., Kim, Y.J., Choi, J.B., and Hong, B.H. (2011). High-performance graphene-based transparent flexible heaters. *Nano Lett.* *11*, 5154–5158.
- Khalid, B., Bai, X., Wei, H., Huang, Y., Wu, H., and Cui, Y. (2017). Direct blow-spinning of nanofibers on a window screen for highly efficient PM_{2.5} removal. *Nano Lett.* *17*, 1140–1148.
- Kim, H., Gilmore, C.M., Pique, A., Horwitz, J.S., Mattoussi, H., Murata, H., Kafafi, Z.H., and Chrisey, D.B. (1999). Electrical, optical, and structural properties of indium-tin-oxide thin films for organic light-emitting devices. *J. Appl. Phys.* *86*, 6451–6461.

- Kim, T., Kim, Y.W., Lee, H.S., Kim, H., Yang, W.S., and Suh, K.S. (2013). Uniformly interconnected silver-nanowire networks for transparent film heaters. *Adv. Funct. Mater.* **23**, 1250–1255.
- Kim, H., Lee, H., Ha, I., Jung, J., Won, P., Cho, H., Yeo, J., Hong, S., Han, S., Kwon, J., et al. (2018). Biomimetic color changing anisotropic soft actuators with integrated metal nanowire percolation network transparent heaters for soft robotics. *Adv. Funct. Mater.* **28**, 1801847.
- Layani, M., Gruchko, M., Milo, O., Balberg, I., Azulay, D., and Magdassi, S. (2009). Transparent conductive coatings by printing coffee ring arrays obtained at room temperature. *ACS Nano* **3**, 3537–3542.
- Lee, K.-S., Lim, J.-W., Kim, H.-K., Alford, T.L., and Jabbour, G.E. (2012). Transparent conductive electrodes of mixed TiO₂-x-indium tin oxide for organic photovoltaics. *Appl. Phys. Lett.* **100**, 213302.
- Lee, H., Hong, S., Lee, J., Suh, Y.D., Kwon, J., Moon, H., Kim, H., Yeo, J., and Ko, S.H. (2016). Highly stretchable and transparent supercapacitor by Ag-Au core-shell nanowire network with high electrochemical stability. *ACS Appl. Mater. Interfaces* **8**, 15449–15458.
- Lee, J., An, K., Won, P., Ka, Y., Hwang, H., Moon, H., Kwon, Y., Hong, S., Kim, C., Lee, C., et al. (2017). A dual-scale metal nanowire network transparent conductor for highly efficient and flexible organic light emitting diodes. *Nanoscale* **9**, 1978–1985.
- Lin, J., Lai, M., Dou, L., Kley, C.S., Chen, H., Peng, F., Sun, J., Lu, D., Hawks, S.A., Xie, C., et al. (2018). Thermochromic halide perovskite solar cells. *Nat. Mater.* **17**, 261–267.
- Liu, B., Zhang, J., Wang, X.F., Chen, G., Chen, D., Zhou, C.W., and Shen, G.Z. (2012). Hierarchical three-dimensional ZnCo₂O₄ nanowire arrays/carbon cloth anodes for a novel class of high-performance flexible lithium-ion batteries. *Nano Lett.* **12**, 3005–3011.
- Liu, J.-W., Huang, W.-R., Gong, M., Zhang, M., Wang, J.-L., Zheng, J., and Yu, S.-H. (2013). Ultrathin hetero-nanowire-based flexible electronics with tunable conductivity. *Adv. Mater.* **25**, 5910–5915.
- Liu, J.-W., Wang, J.-L., Wang, Z.-H., Huang, W.-R., and Yu, S.-H. (2014). Manipulating nanowire assembly for flexible transparent electrodes. *Angew. Chem. Int. Ed.* **53**, 13477–13482.
- Liu, C., Hsu, P.C., Lee, H.W., Ye, M., Zheng, G., Liu, N., Li, W., and Cui, Y. (2015). Transparent air filter for high-efficiency PM_{2.5} capture. *Nat. Commun.* **6**, 6205.
- Moon, H., Lee, H., Kwon, J., Suh, Y.D., Kim, D.K., Ha, I., Yeo, J., Hong, S., and Ko, S.H. (2017). Ag/Au/polypyrrole core-shell nanowire network for transparent, stretchable and flexible supercapacitor in wearable energy devices. *Sci. Rep.* **7**, 41981.
- Parkin, I.P., and Manning, T.D. (2006). Intelligent thermochromic windows. *J. Chem. Educ.* **83**, 393–400.
- Seeboth, A., Löttsch, D., Ruhmann, R., and Muehling, O. (2014). Thermochromic polymers function by design. *Chem. Rev.* **114**, 3037–3068.
- Sui, D., Huang, Y., Huang, L., Liang, J., Ma, Y., and Chen, Y. (2011). Flexible and transparent electrothermal film heaters based on graphene materials. *Small* **7**, 3186–3192.
- Tokuno, T., Nogi, M., Jiu, J., Sugahara, T., and Sugauma, K. (2012). Transparent electrodes fabricated via the self-assembly of silver nanowires using a bubble template. *Langmuir* **28**, 9298–9302.
- Wang, X., Zhi, L., and Muellen, K. (2008). Transparent, conductive graphene electrodes for dye-sensitized solar cells. *Nano Lett.* **8**, 323–327.
- Wu, J., Agrawal, M., Becerril, H.A., Bao, Z., Liu, Z., Chen, Y., and Peumans, P. (2010). Organic light-emitting diodes on solution-processed graphene transparent electrodes. *ACS Nano* **4**, 43–48.
- Wu, H., Kong, D., Ruan, Z., Hsu, P.-C., Wang, S., Yu, Z., Carney, T.J., Hu, L., Fan, S., and Cui, Y. (2013). A transparent electrode based on a metal nanotrough network. *Nat. Nanotechnol.* **8**, 421–425.
- Xu, J., Liu, C., Hsu, P.C., Liu, K., Zhang, R., Liu, Y., and Cui, Y. (2016). Roll-to-roll transfer of electrospun nanofiber film for high-efficiency transparent air filter. *Nano Lett.* **16**, 1270–1275.
- Yang, C., Gu, H., Lin, W., Yuen, M.M., Wong, C.P., Xiong, M., and Gao, B. (2011). Silver nanowires: from scalable synthesis to recyclable foldable electronics. *Adv. Mater.* **23**, 3052–3056.
- Yoon, Y.-H., Song, J.-W., Kim, D., Kim, J., Park, J.-K., Oh, S.-K., and Han, C.-S. (2007). Transparent film heater using single-walled carbon nanotubes. *Adv. Mater.* **19**, 4284–4287.
- Zhang, D., Ryu, K., Liu, X., Polikarpov, E., Ly, J., Tompson, M.E., and Zhou, C. (2006). Transparent, conductive, and flexible carbon nanotube films and their application in organic light-emitting diodes. *Nano Lett.* **6**, 1880–1886.
- Zhang, R., Liu, C., Hsu, P.-C., Zhang, C., Liu, N., Zhang, J., Lee, H.R., Lu, Y., Qiu, Y., Chu, S., et al. (2016). Nanofiber air filters with high-temperature stability for efficient PM_{2.5} removal from the pollution sources. *Nano Lett.* **16**, 3642–3649.
- Zheng, J., Bao, S., and Jin, P. (2015). TiO₂(R)/VO₂(M)/TiO₂(A) multilayer film as smart window: combination of energy-saving, antifogging and self-cleaning functions. *Nano Energy* **11**, 136–145.
- Zhou, C., Gao, T., Wang, Y., Liu, Q., Huang, Z., Liu, X., Qing, M., and Xiao, D. (2018). Synthesis of P-doped and NiCo-hybridized graphene-based fibers for flexible asymmetrical solid-state micro-energy storage device. *Small* **15**, 1803469.

ISCI, Volume 12

Supplemental Information

**Mass Production of Nanowire-Nylon
Flexible Transparent Smart Windows
for PM_{2.5} Capture**

Wei-Ran Huang, Zhen He, Jin-Long Wang, Jian-Wei Liu, and Shu-Hong Yu

1. Table S1. Unit prices of the chemicals which have been used in our experiment, Related to Figure 1.

Chemicals	AgNO ₃	Glycerol	H ₂ O	NaCl	PVP
Unit price	0.427 dollar g ⁻¹	4.64 dollars L ⁻¹	1.20 dollars L ⁻¹	1.82 dollars kg ⁻¹	0.039 dollar g ⁻¹

2. Cost accounting of Ag-nylon electrodes, Related to Figure 1.

The cost accounting in this manuscript includes the cost of chemicals, commercial nylon, labor and energy.

(1). the cost of energy. It take us 0.016 dollar for 180 W heating devices worked for about 1 h.

According to the Ag nanowire synthesis section mentioned above, it takes us 2.342 dollars for 1g Ag nanowires.

(2). the price of commercial nylon mesh was 0.137 dollar m⁻².

(3). For the fabrication process of large-scale Ag-nylon mesh (7.5 m²), one people would spend 0.33 h to complete it and the labor cost was 1.43 dollars h⁻¹ in Hefei.

(4). It takes 2.01 dollars to fabricate 1 m² Ag-nylon electrodes with the transmittance was 86.05% and conductivity of 8.87 Ω sq⁻¹ which contains 0.769 g Ag nanowires.

Supplemental Figures

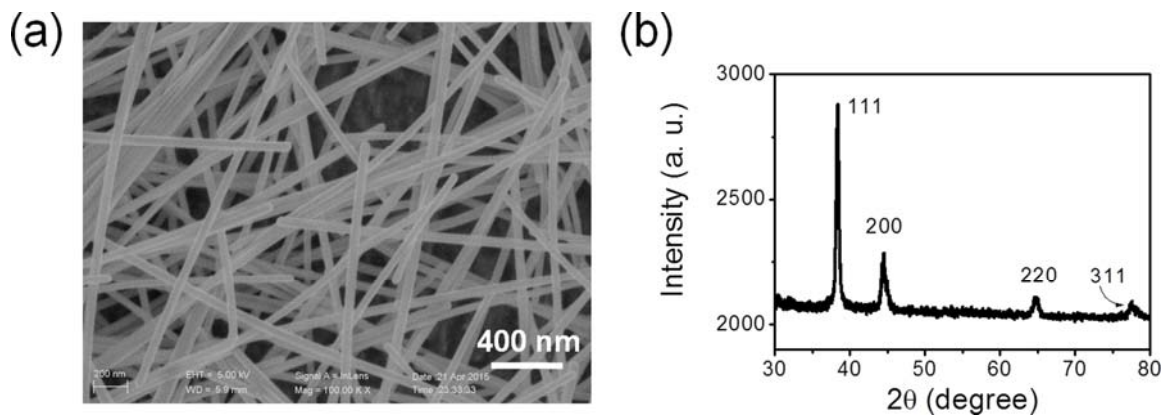


Figure S1. SEM image and XRD spectrum of Ag nanowires, Related to Figure 1.

(a) SEM image of Ag nanowires. (b) XRD spectrum of Ag nanowires.

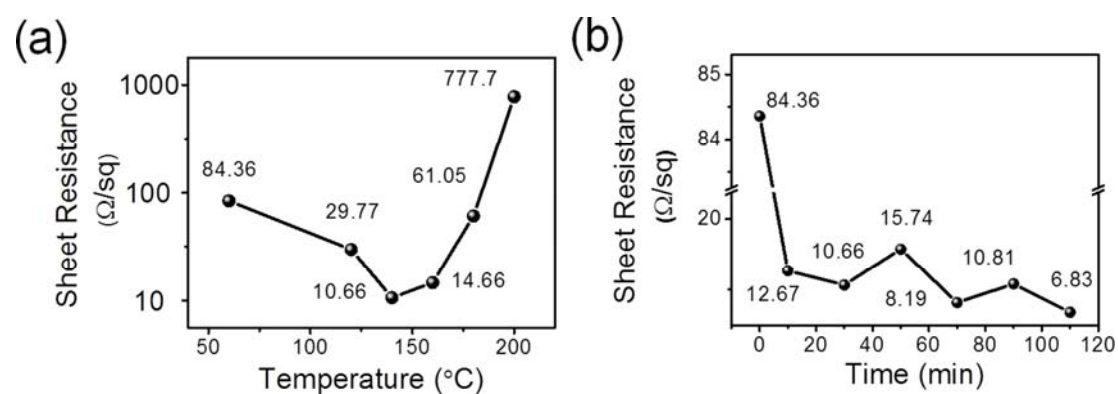


Figure S2. Influence of temperature and heating time on the conductivity of Ag-nylon electrodes, Related to Figure 2.

(a) Sheet resistance of conductive Ag-nylon electrodes as a function of different temperature for 15 minutes. (b) Sheet resistance of conductive Ag-nylon electrodes as a function of different reaction time at 140 °C.

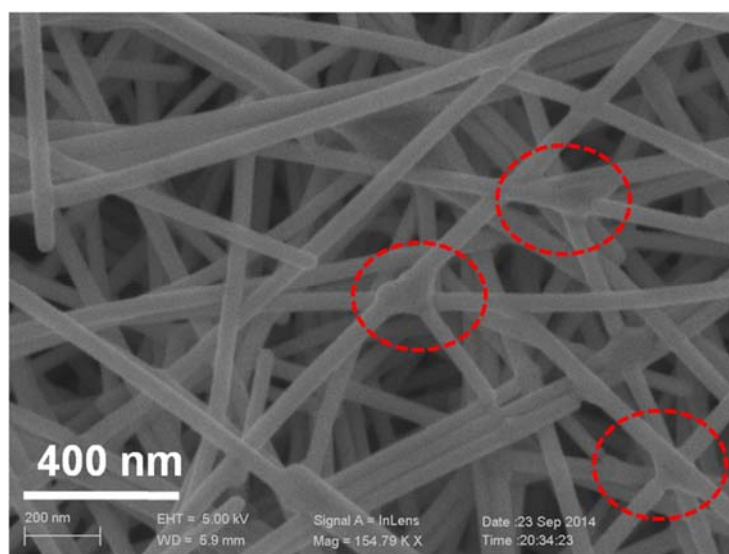


Figure S3. The SEM images of Ag-nylon electrode after 15 min annealing process under 140 °C, Related to Figure 2.

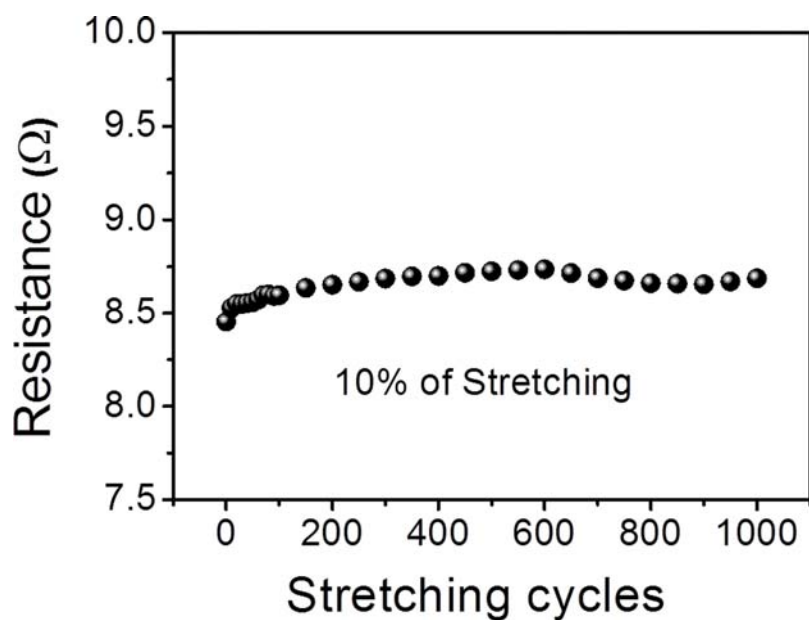


Figure S4. Resistance responses of 10% tensile strain as function of stretching cycles, Related to Figure 2.

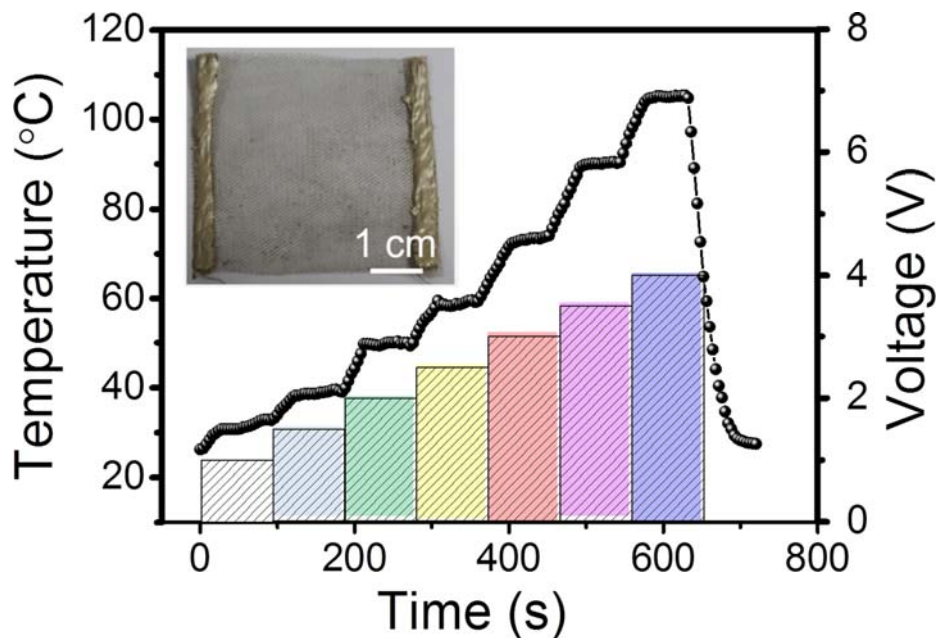


Figure S5. Temperature profiles with consecutive inputs of regular square wave voltages from 1.0, 1.5, 2.0, 2.5, 3.0, 3.5 and 4.0 V, Related to Figure 3. Inset is optical image of an Ag-nylon flexible transparent heaters.

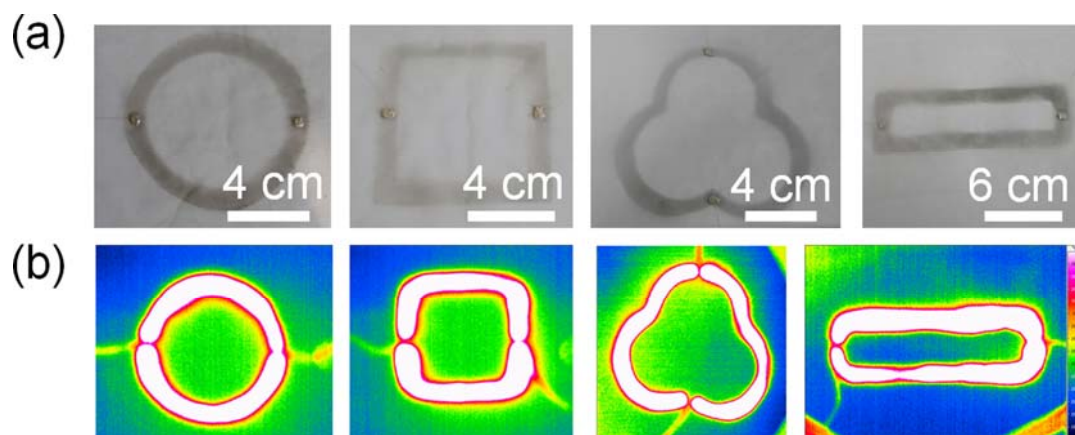


Figure S6. The uniform heating performance of different conductive patterns, Related to Figure 3. (a, b) Optical images and infrared pictures of Ag-nylon patterns with the different shapes showing their uniform heat distribution and outstanding design flexibility.

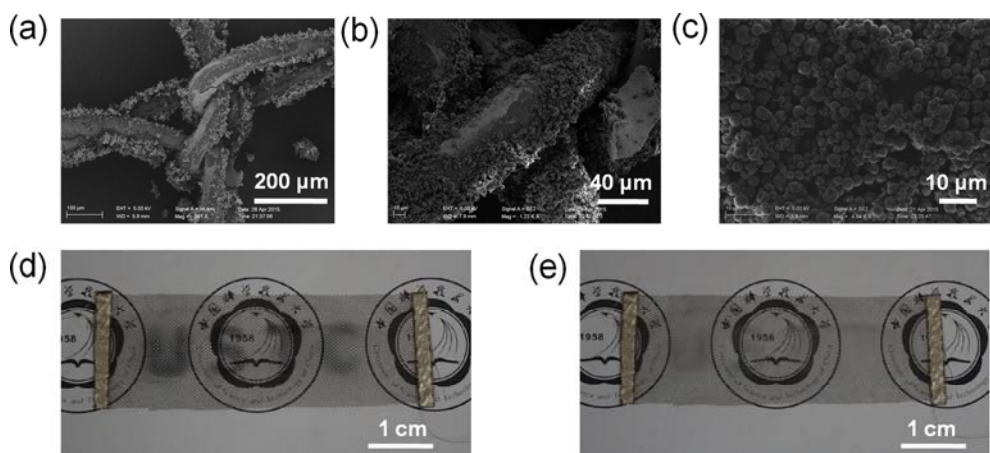


Figure S7. Ag-nylon electrodes coating with variable thermochromic dye, Related to Figure 3. (a-c) SEM images of conductive meshes coating with variable thermochromic dye powder with different magnifications. (d-e) Photographs of the variation of conductive mesh's transmittance during thermochromic experiment. (d) Before, and (e) after heating the Ag-nylon mesh coating with thermochromic dye powder.

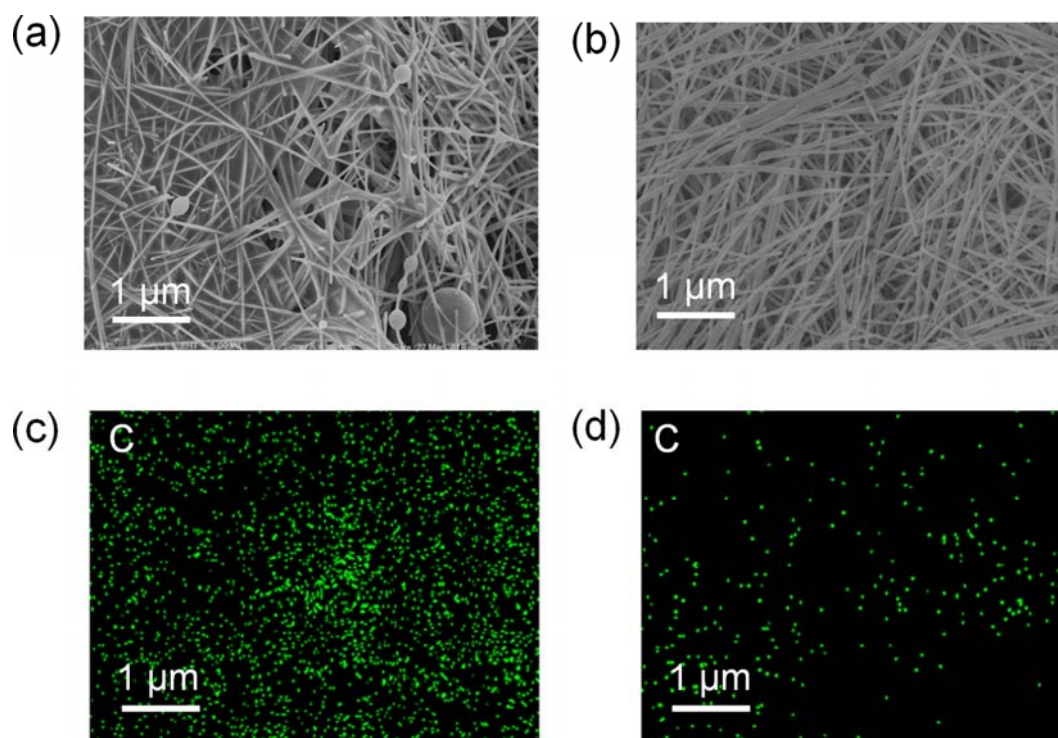


Figure S8. The SEM and EDX mapping images of carbon content for the PM material before and after cleaning, Related to Figure 4. (a, c) before cleaning. (b, d) after cleaning.

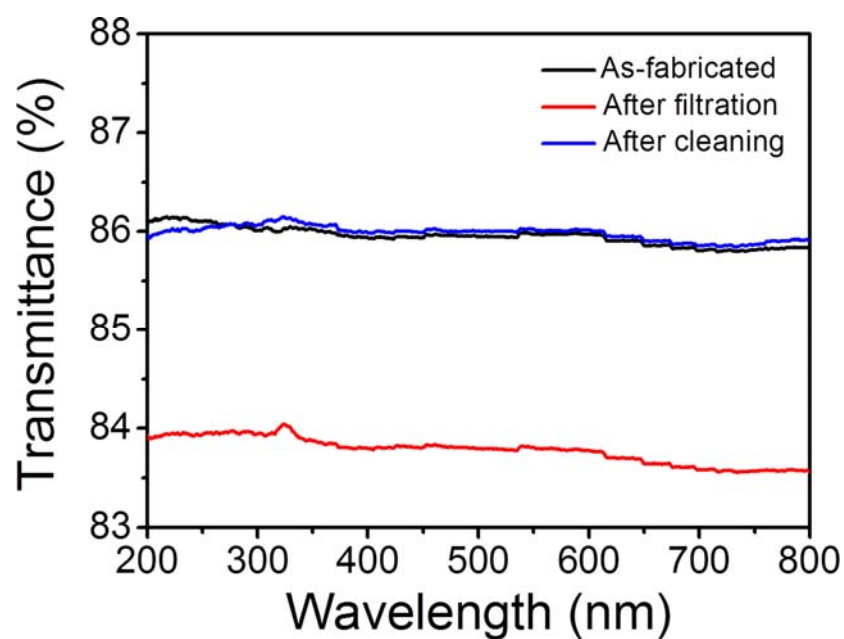


Figure S9. Optical transmittance of Ag-nylon mesh as PM filter during PM filtration process and cleaning process, Related to Figure 4.



Figure S10. Photographs of Ag-nylon electrode as PM filter, Related to Figure 4. (a) as-fabricated, (b) after PM filtration and (c) after cleaning process.

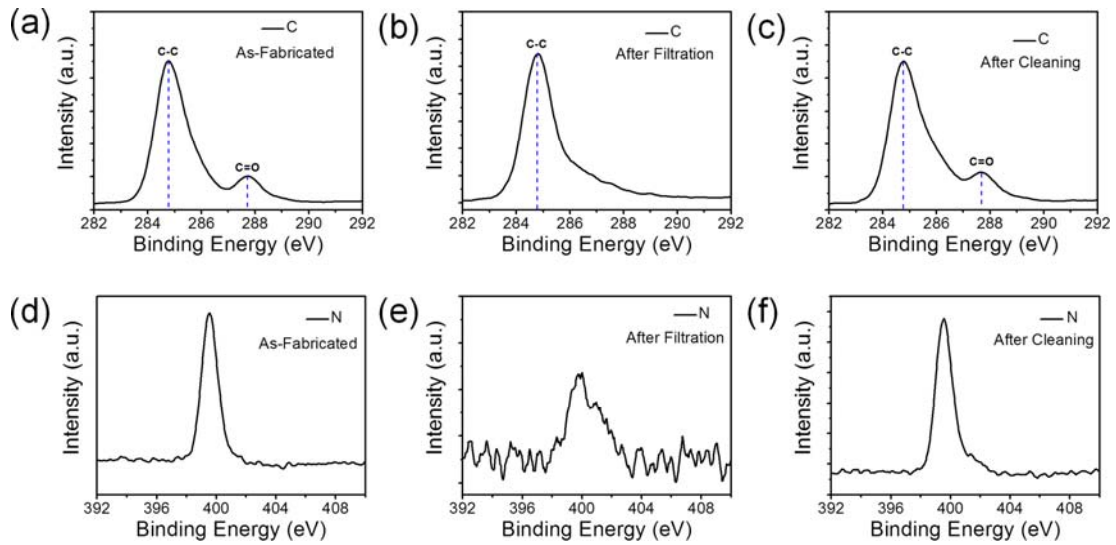


Figure S11. X-ray photoelectron spectroscopy (XPS) spectrum of Ag-nylon meshes for PM filtration experiment, Related to Figure 4. (a-c) XPS characterization for carbon peaks of Ag-nylon mesh, Ag-nylon mesh after PM filtration, and Ag-nylon mesh after cleaning process respectively. (d-f) XPS characterization for nitrogen peaks of Ag-nylon mesh, Ag-nylon mesh after PM filtration, and Ag-nylon mesh after cleaning process respectively.

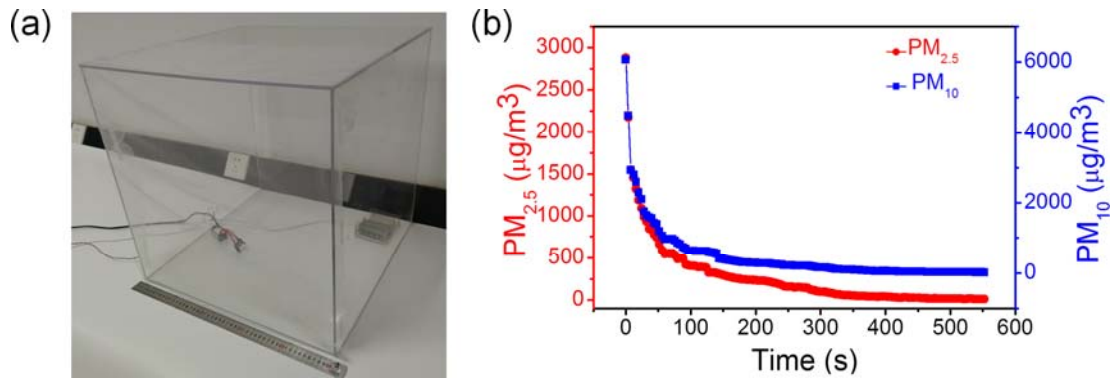


Figure S12. Large-scale PM filtration experiment, Related to Figure 4. (a) Optical image of the experiment setup of PM filtration in large cube. (b) The performance of PM filtration in large cube with the side length of 0.5 m under the voltage of 10 V.

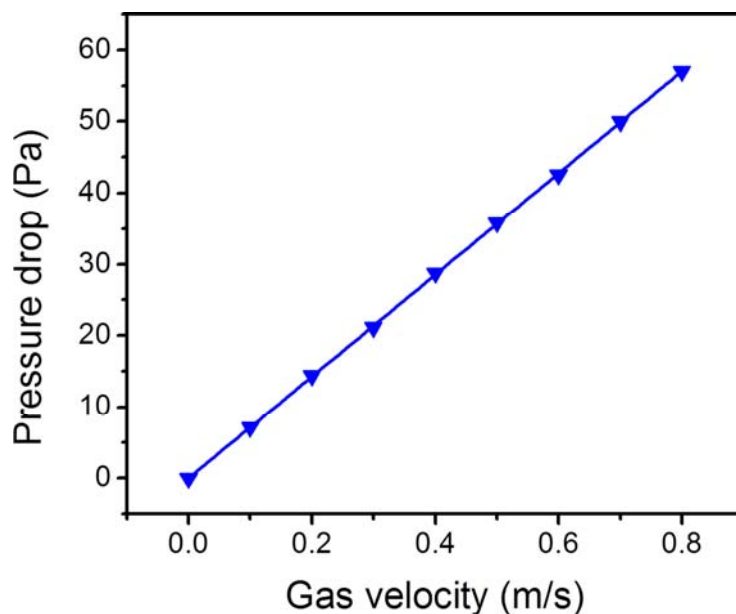


Figure S13. The pressure drop of PM filter, Related to Figure 4.

Movie S1. Preparation process of Ag-nylon electrode, Related to Figure 1.

Movie S2. Ag-nylon thermochromic devices, Related to Figure 3.

Transparent Methods

Materials

All chemicals are of analytical grade, which are commercially available from Sinopharm Chemical Reagent Co., Ltd and are used in this experiment without further purification.

Synthesis of Ag NWs

The Ag nanowires were synthesized using the method reported previously (Adv. Mater. 23, 3052-3056). In a typical synthesis, 180 mL of glycerol (99%) and 5.54 g of Poly (vinyl pyrrolidone) (PVP, $M_w \approx 40,000$) were mixed in a three-necked round-bottom flask with vigorous magnetic stirring at 110 °C for 30 minutes. After temperature dropped down to 60 °C naturally, 10 mL of glycerol solution containing 0.47 mL of H₂O and 56 mg of sodium chloride (NaCl, 99%) was added into the flask under vigorous magnetic stirring for 5 minutes. Then 1.58 g of silver nitrate (AgNO₃, 99.5%) was added into the solution quickly with gentle stirring (60 rpm). Subsequently, the reaction temperature was raised from 60 °C to 210 °C in 30 minutes. It could be found that the color of the solution turned from milky into light brown,

brownish red, dark gray and eventually gray-green. When the temperature reached 210 °C, the heating process was forced to stop. Firstly, the solution was poured into 500 mL beaker immediately, and then deionized water was added into the solution in 1: 1 ratio to low the temperature. After the synthesis, the product was placed in room temperature for two days. After removing the supernatant layer, the precipitate of Ag NWs was collected and dispersed into an ethanol solution with the concentration of 3.92 mg mL⁻¹.

Preparation of conductive Ag-nylon electrodes

The flexible transparent conductive Ag-nylon electrodes were prepared by simply immersing nylon meshes in Ag nanowire solution. Firstly, 20 mL of Ag nanowire solution was washed by ethanol two times to remove PVP surfactant and glycerol solvent. Then, Ag nanowire was dispersed in ethanol in a big glass culture dish. Before the fabrication procedure, commercial nylon was cleaned by alcohol and acetone in turn, then ultrasonic treatment for 30 min and dried in 60 °C. The nylon mesh was immersed in the Ag nanowire solution for 30 s and dried in the air at room temperature. With the amount of the dipping coating cycles increasing, the bare nylon mesh was gradually coated with a film of Ag nanowires. Finally, the obtained Ag-nylon mesh was heat at 140 °C for 15 minutes in air.

Fabrication of thermochromic device

Thermochromic dye (a mixture of crystalline violet lipid, bisphenol A and hexadecanol was added in one independent small SiO₂ sphere with content ratio of 1:3:50.) was purchased from Zhongshan Jiahua Company and the temperature of the color transformation is 33 °C. Ag-nylon electrodes coating with variable color dye were fabricated through spraying method. Firstly, one square conductive mesh (5 cm × 5 cm) was put on the heating platform. 0.2 g of thermochromic dye powder was dispersed in 10 mL acetone under vigorous shaking for 10 minutes. The dispersion as prepared was poured into an airbrush and sprayed to conductive mesh under continuous heating at 60 °C. Various molds with different shapes can be covered on conductive meshes before spraying process to make thermochromic devices have different patterns.

Fabrication of conductive Ag-nylon patterns

The silica gel boards with different shape and size were used as mask to make different patterns. Firstly, the silica gel mask was covered on the nylon mesh and 10 mL of Ag NWs ethanol solution with the concentration of 3.92 mg mL⁻¹ was sprayed to the pattern with spray gun. In this process, the silica gel mask and nylon mesh were heated to 80 °C to dry the solvent and the spray gun worked in air.